

# Benzodithiophene based $\pi$ -conjugated macrocycle: synthesis, morphology and electrochemical characterization

Anjan Bedi,\* Sanjio S. Zade\*

Department of Chemical Sciences, Indian Institute of Science Education and Research (IISER)  
Kolkata, Mohanpur 741246, India.

[\*] email: [sanjiozade@iiserkol.ac.in](mailto:sanjiozade@iiserkol.ac.in), [anjan.bedi@gmail.com](mailto:anjan.bedi@gmail.com)

Contents	Page number
<b>Figure S1.</b> $^1\text{H}$ NMR of reported compound <b>3</b>	S2
<b>Figure S2.</b> $^{13}\text{C}$ NMR of reported compound <b>3</b>	S3
<b>Figure S3.</b> $^1\text{H}$ NMR of newly synthesized compound <b>4</b>	S4
<b>Figure S4.</b> $^{13}\text{C}$ NMR of newly synthesized compound <b>4</b>	S5
<b>Figure S5.</b> $^1\text{H}$ NMR of newly synthesized compound <b>5</b>	S6
<b>Figure S6.</b> $^{13}\text{C}$ NMR of newly synthesized compound <b>5</b>	S7
<b>Figure S7.</b> MALDI-TOF mass spectrometry of <b>5</b>	S8
<b>Figure S8.</b> UV-vis spectra of the macrocycle ( <b>5</b> ) in various solvents	S8
<b>Figure S9.</b> (a) Micrograph on a glass plate using a light microscope with 1000 $\times$ magnification. (b) AFM topography of a single fibre obtained on $\text{SiO}_2$ surface. (c) SEM images of single microfiber of the macrocycle on a silicon wafer with 44000 $\times$ magnification (right).	S9
<b>Table 1.</b> NICS (0 to 2 and 0 to -2) value calculated at B3LYP/6-311+G(d,p) on the optimized structure of macrocycle <b>5</b> at B3LYP/6-31G(d).	S9
<b>Figure S10.</b> Optimized structure of the frontier orbitals; (a) HOMO and (b) LUMO of the macrocycle	S10
<b>Fig. S11</b> Decay of fluorescence for compound <b>5</b> in solution (49.06 $\mu\text{M}$ ) and thin film on ITO-coated glass.	S10
<b>Fig. S12</b> Concentration dependent fluorescence spectra of <b>5</b> in THF.	S11
<b>Fig. S13</b> Time-dependent absorption (left) and fluorescence (right) spectra of macrocycle <b>5</b> in THF.	S11
<b>Fig. S14</b> Powder XRD pattern of compound <b>5</b> .	S11
Coordinates for optimized geometry of <b>5</b> at B3LYP/6-31G(d) with optimized energy value	S12
Reference 28 in full	S13

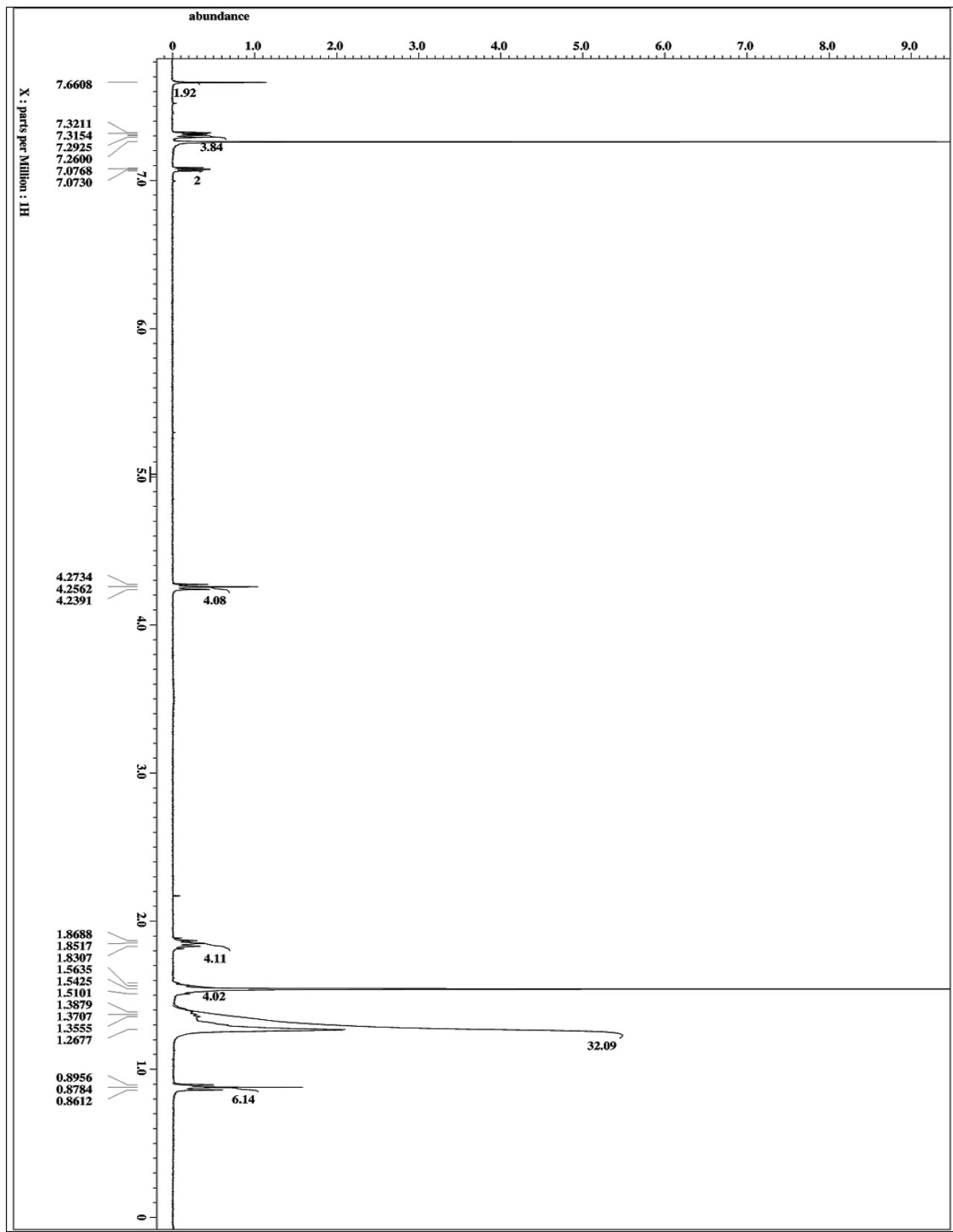


**Fig. S1** <sup>1</sup>H NMR of compound 3

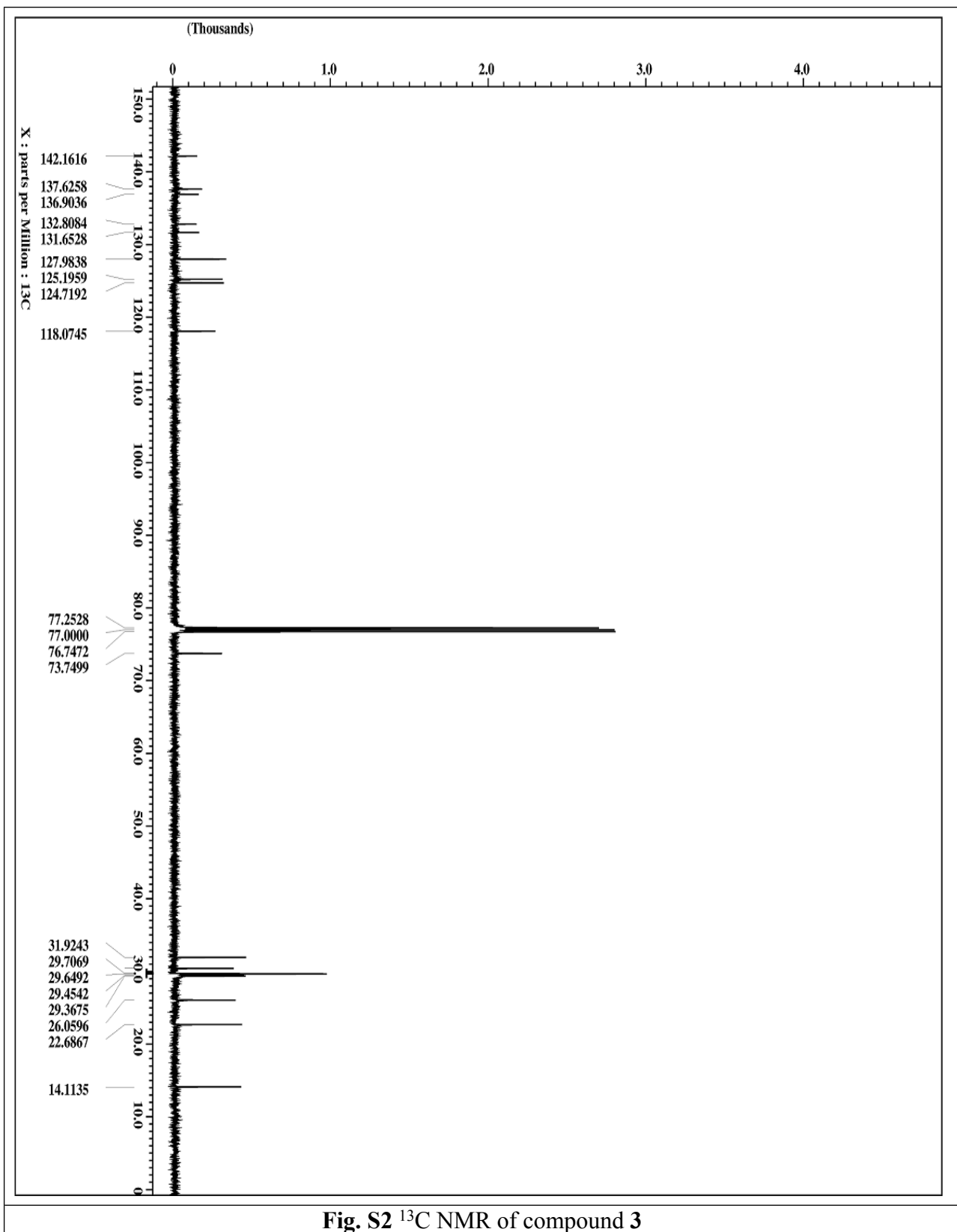
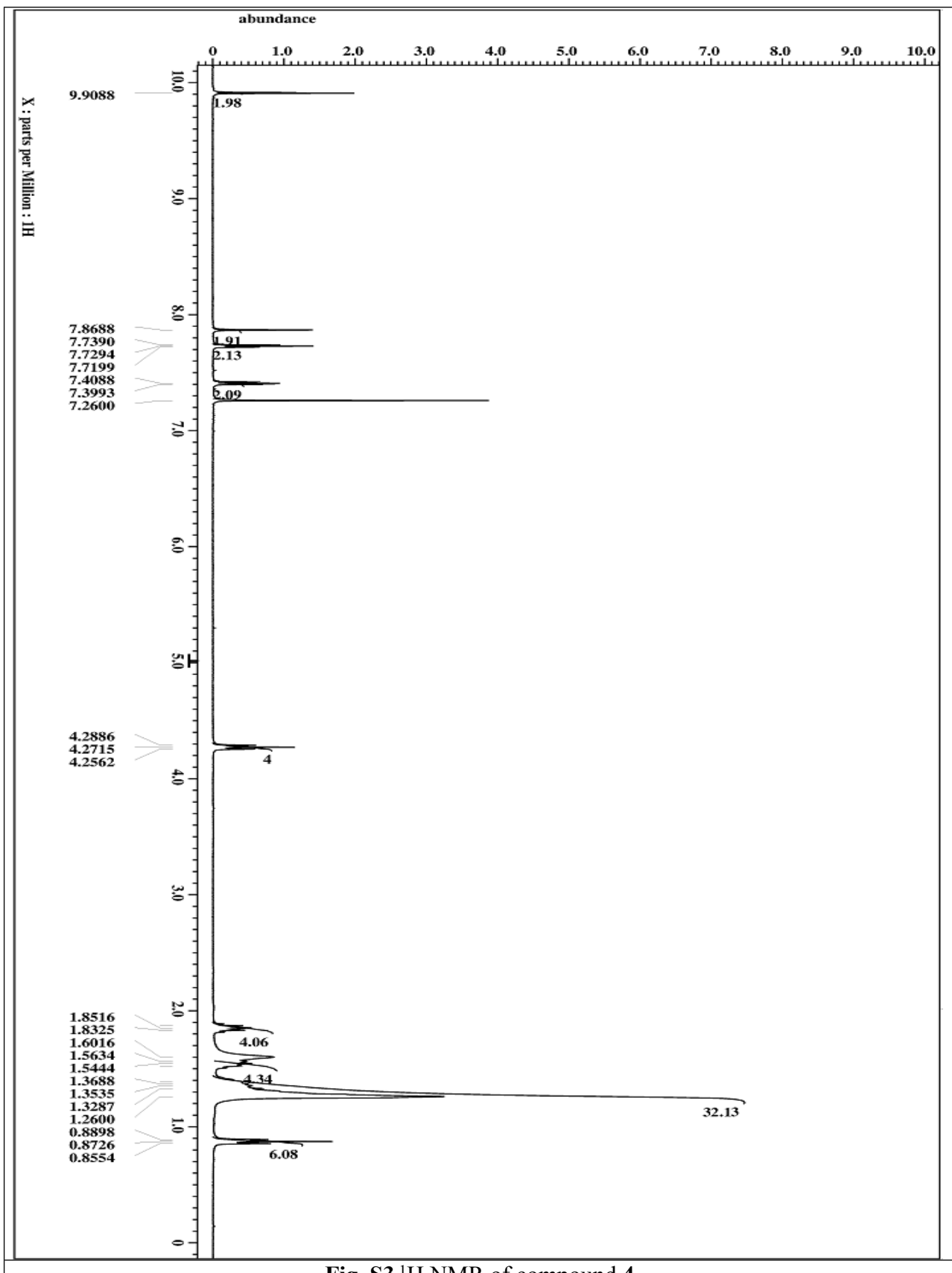


Fig. S2 <sup>13</sup>C NMR of compound 3



**Fig. S3**  $^1\text{H}$  NMR of compound 4

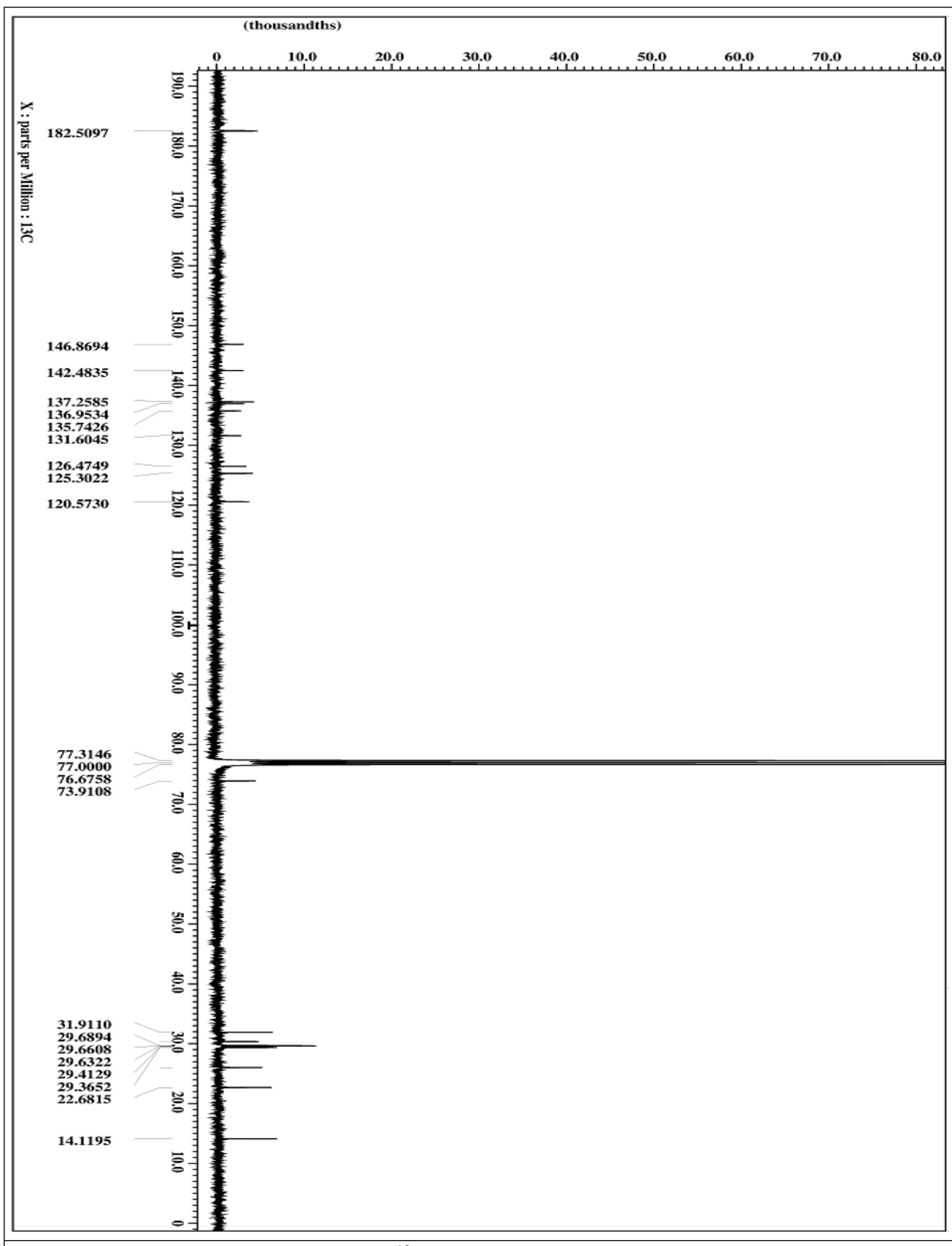
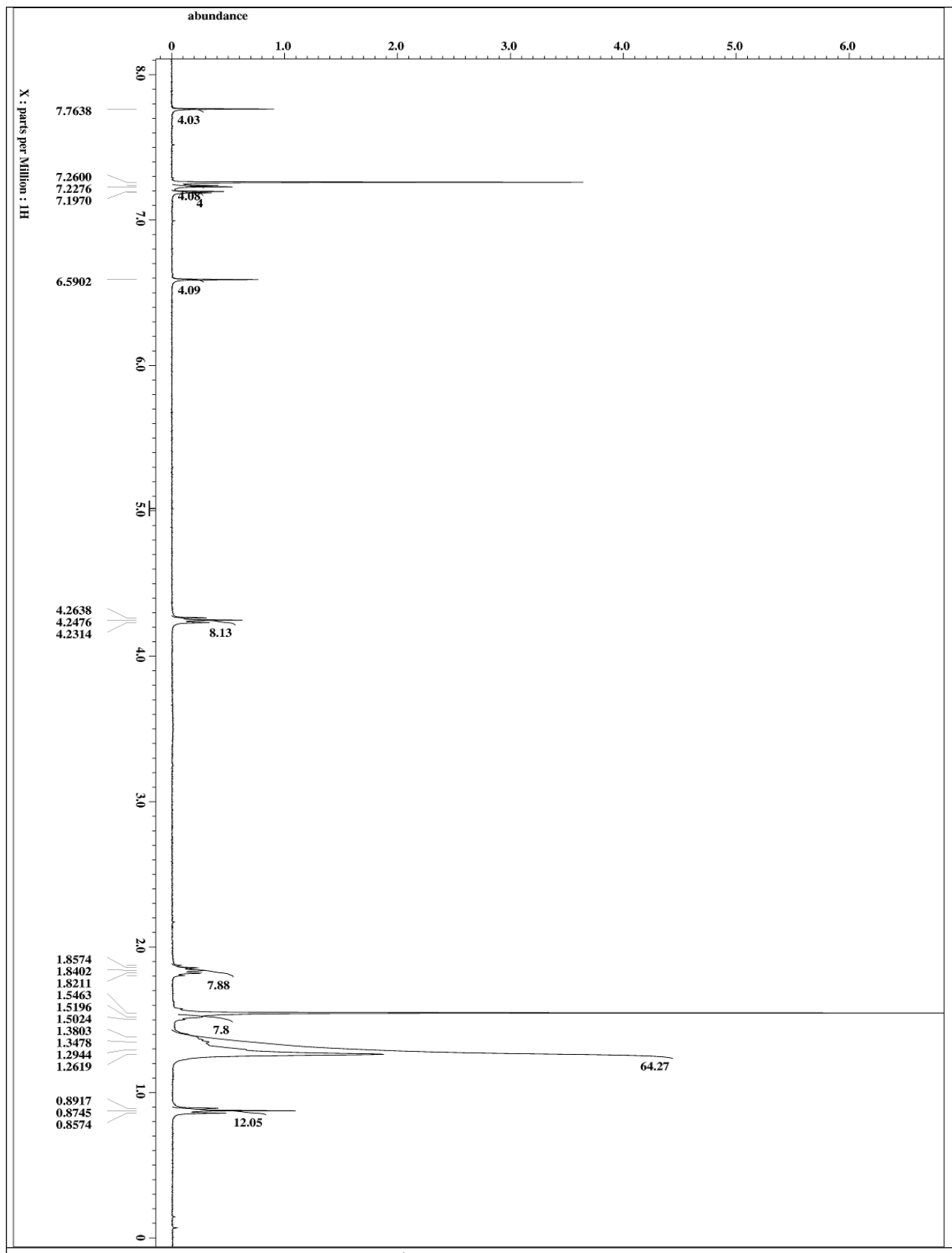


Fig. S4  $^{13}\text{C}$  NMR of compound 4



**Fig. S5**  $^1\text{H}$  NMR of compound 5

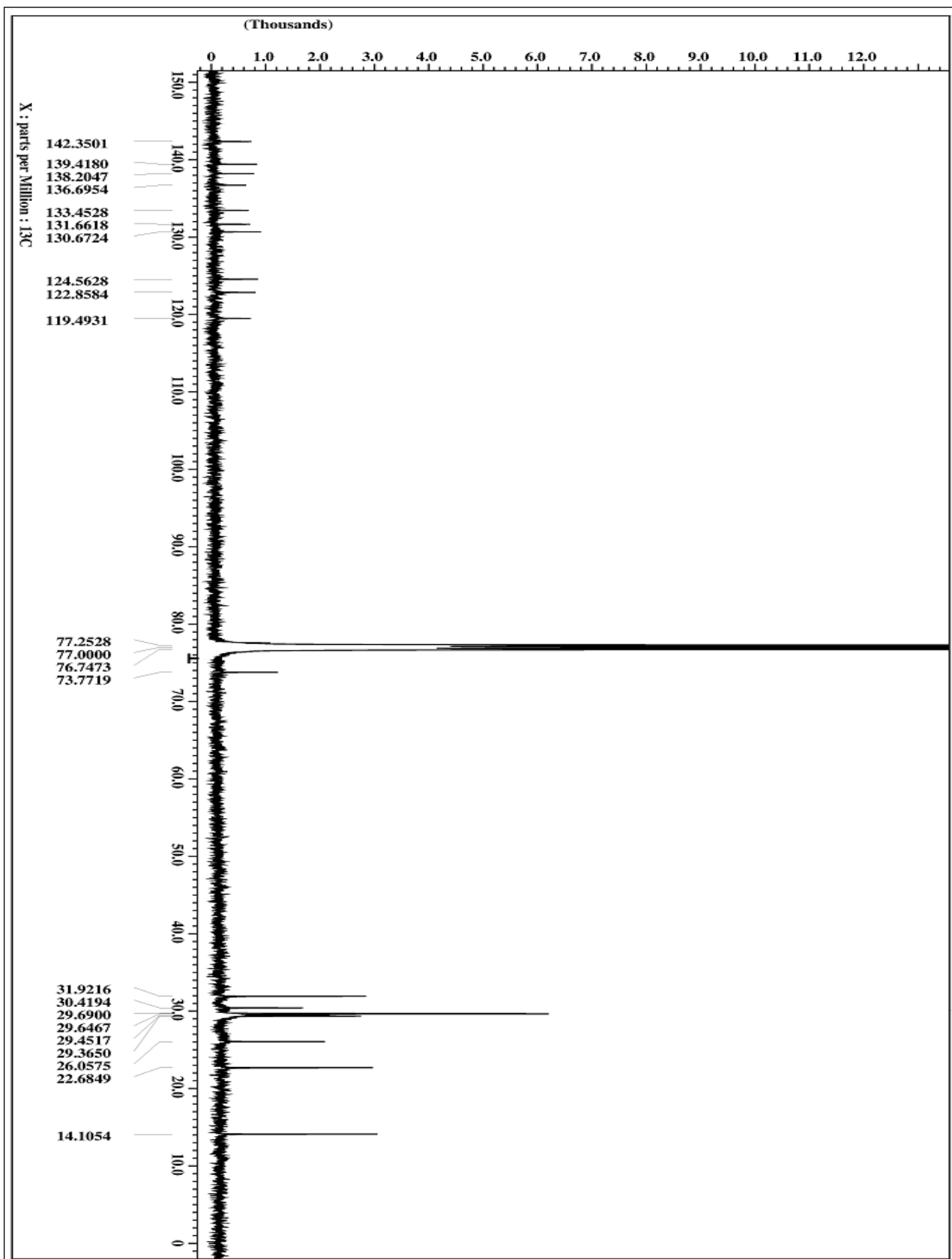


Fig. S6  $^{13}\text{C}$  NMR of compound 5

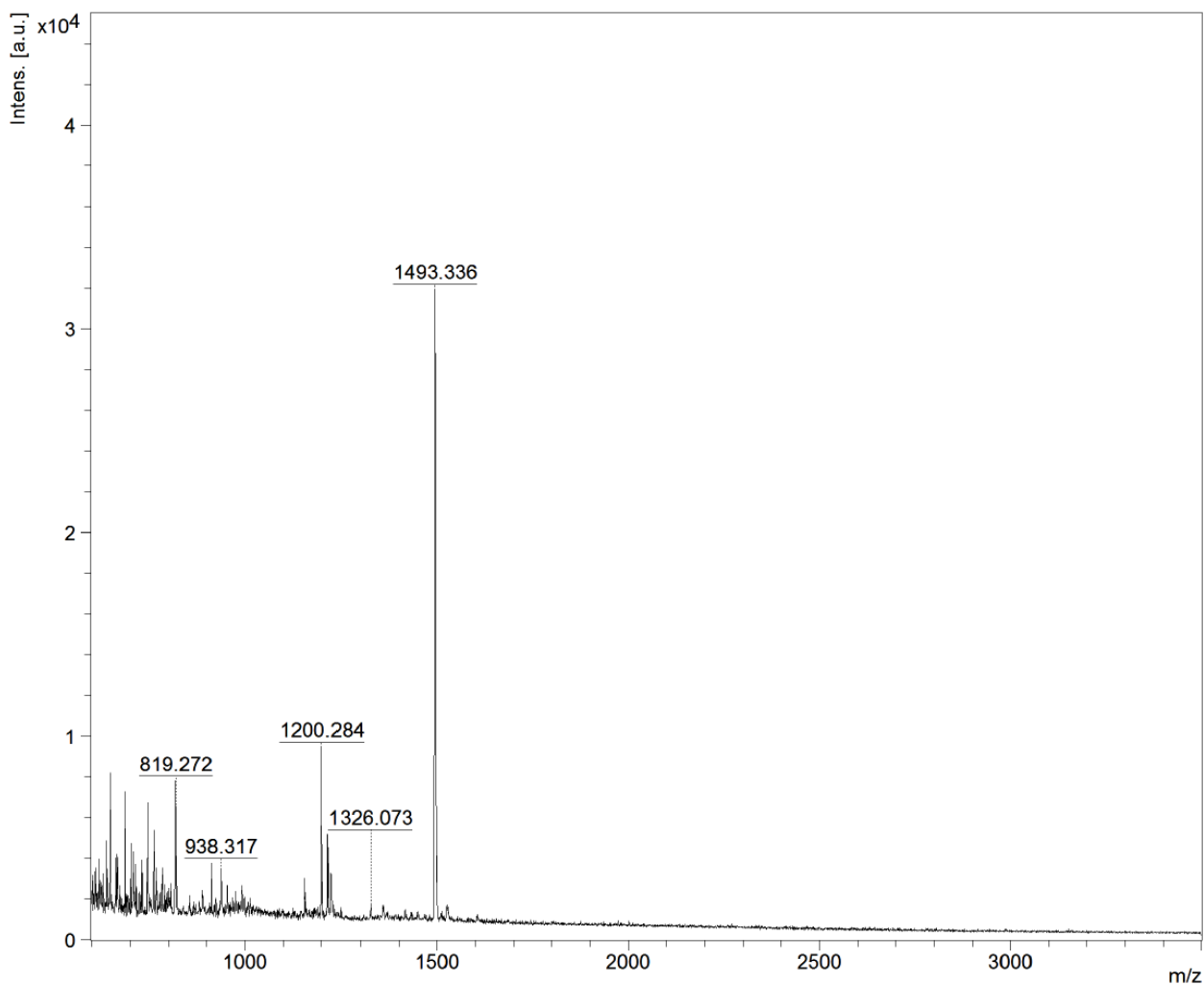


Fig. S7 MALDI-TOF Mass spectrometry of **5**

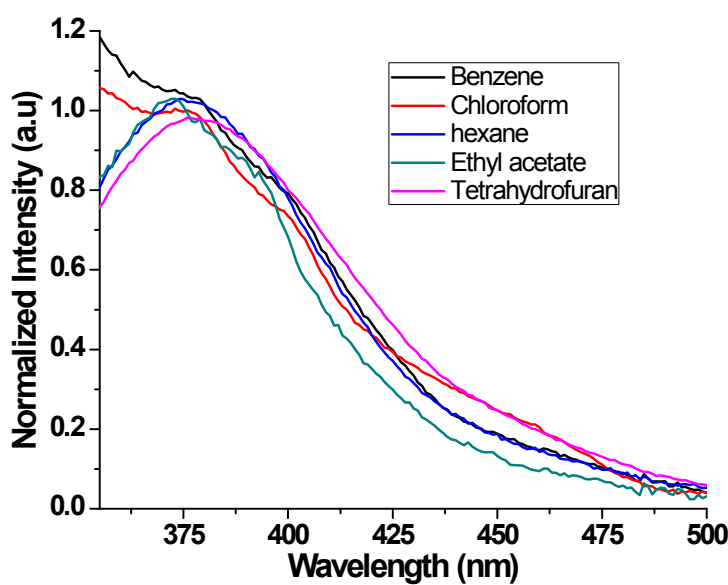
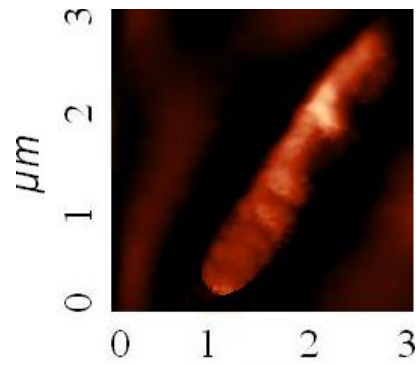
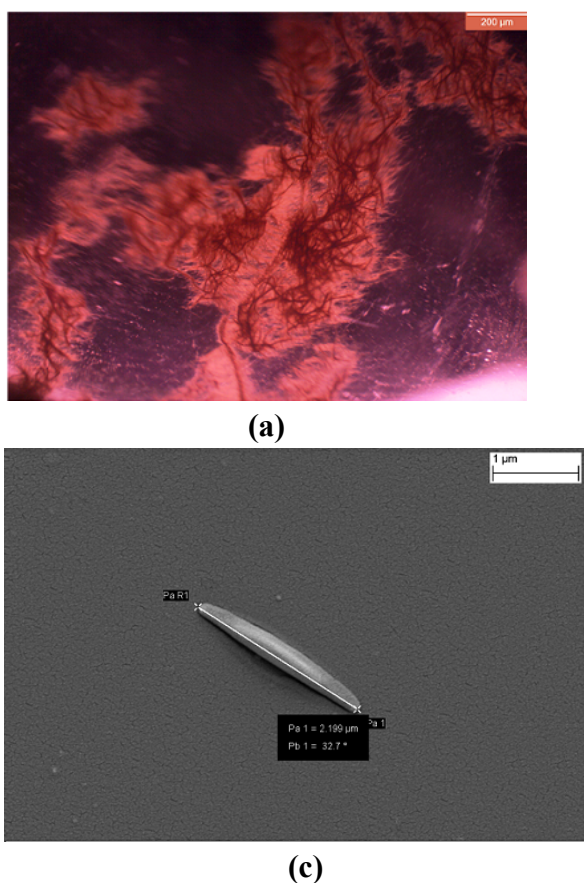


Fig. S8 UV-vis spectra of the macrocycle (**5**) in various solvents.



(b)

(a)

(c)

**Fig. S9** (a) Micrograph on a glass plate using a light microscope with 1000 $\times$  magnification. (b) AFM topography of a single fibre obtained on SiO<sub>2</sub> surface. (c) SEM images of single microfiber of the macrocycle on a silicon wafer with 44000  $\times$  magnification (right).

**Table S1** NICS (0 to 2 and 0 to -2) value calculated at B3LYP/6-311+G(d,p) on the optimized structure of macrocycle **5** at B3LYP/6-31G(d).<sup>a</sup>

Position of Bq	0	1	2	-1	-2
NICS value	1.7	1.6	1.2	1.3	0.7

<sup>a</sup> The coordinates of Bq(0) to get NICS(0) was calculated by averaging the coordinates of four hydrogen and four sulfur atoms of the inside periphery of the macrocycle **5**. Bq(1, 2, -1, -2) were placed with respect to Bq(0).

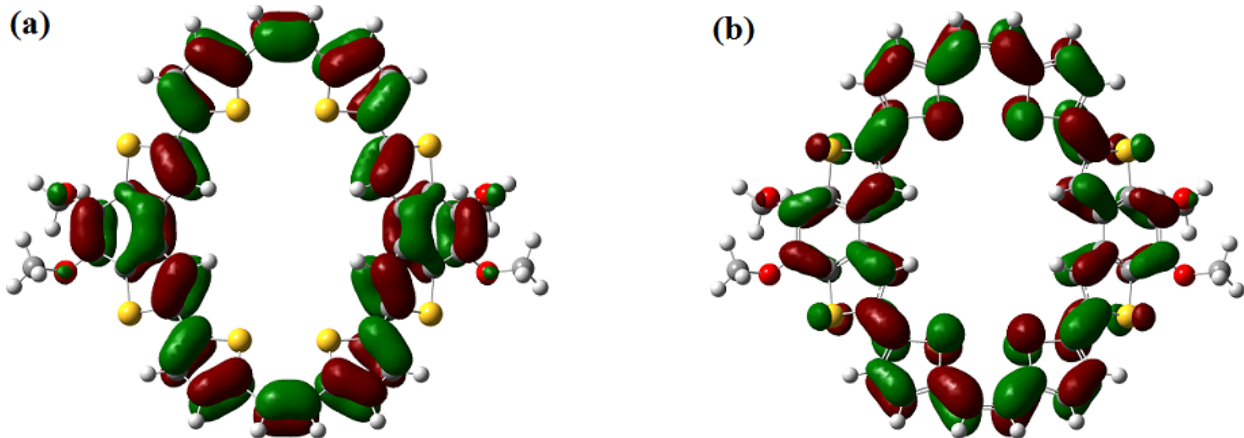


**Fig. S10** Optimized structure of the frontier orbitals; (a) HOMO and (b) LUMO of the macrocycle.

#### Fluorescence decay:

The fluorescence decay for compound **5** was also studied to confirm the formation of the excimer. This needed a single exponential fit in solution but required a double exponential fit in solid state. In solution, a sole component of **5** with a lifetime ( $\tau_1$ ,  $x^2 = 1.26$ ) of 1.15 ns was present. But, in film two components were present with lifetime of 445 ps ( $\tau_1$ , 37%,  $x^2 = 1.17$ ) and 1.12 ns ( $\tau_2$ , 63%,  $x^2 = 1.17$ ). As the higher lifetime is believed to be found from the excimer species, the excimers dominated the fluorescent behavior of the compound in solid to shift the  $\lambda_{max}^{em}$  by 200 nm to the lower energy.

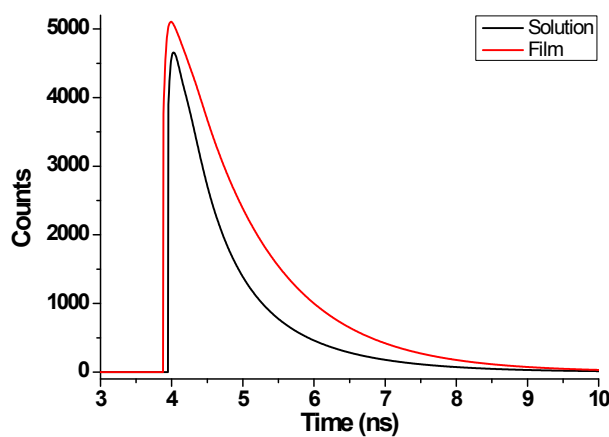


**Fig. S11** Decay of fluorescence for compound **5** in solution (49.06  $\mu$ M) and thin film on ITO-coated glass.

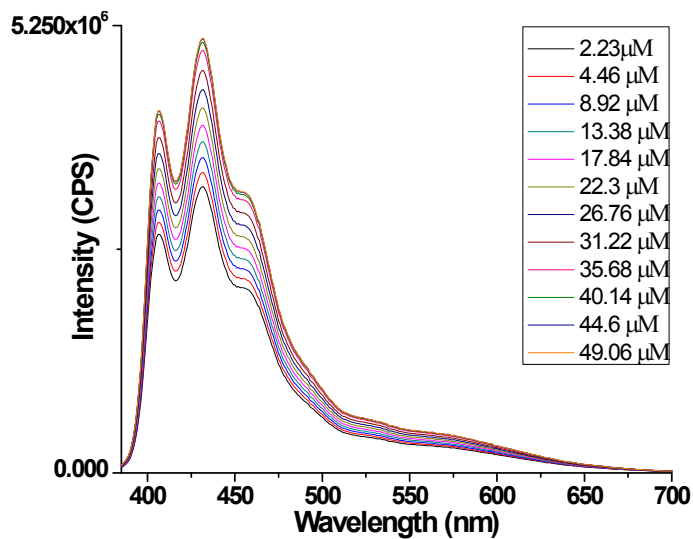


**Fig. S12** Concentration dependent fluorescence spectra of **5** in THF.

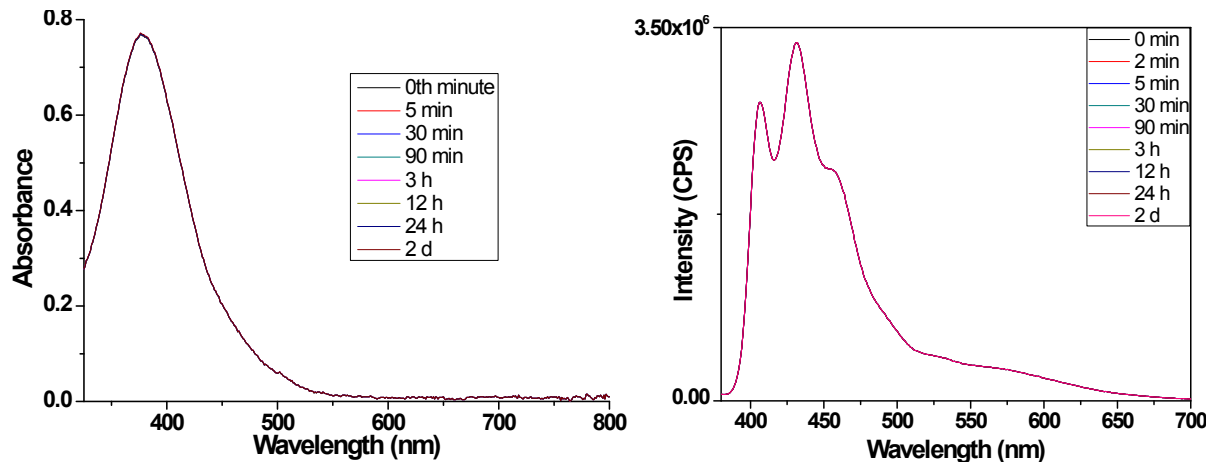


**Fig. S13** Time-dependent absorption (left) and fluorescence (right) spectra of macrocycle **5** in THF.

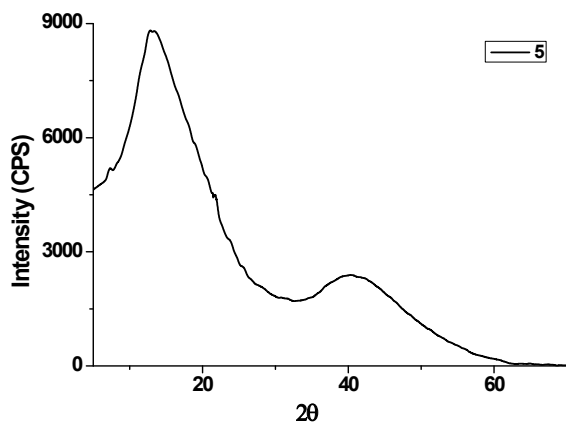


**Fig. S14** Powder XRD pattern of compound **5**

## Coordinates for optimized geometry of 5 at B3LYP/6-31G(d)

Center Number	Atomic Number	Atomic Type	Coordinates (Angstroms)		
			X	Y	Z
1	6	0	-5.701480	1.364236	0.815192
2	6	0	-4.595882	0.710376	0.227023
3	6	0	-3.657474	1.643719	-0.319830
4	6	0	-4.032895	2.955895	-0.169483
5	6	0	-6.785758	0.685042	1.396778
6	6	0	-4.599742	-0.713365	0.206384
7	6	0	-5.698393	-1.378830	0.794448
8	6	0	-6.773375	-0.711058	1.406377
9	6	0	-4.033287	-2.951277	-0.226025
10	6	0	-3.662619	-1.636085	-0.360482
11	1	0	-2.756061	1.350814	-0.847503
12	1	0	-2.765428	-1.333248	-0.889738
13	16	0	-5.562420	-3.115525	0.652647
14	16	0	-5.565369	3.103454	0.706552
15	6	0	-3.385557	-4.150147	-0.712340
16	6	0	-3.984283	-5.347956	-1.054680
17	16	0	-1.648835	-4.249806	-0.937808
18	6	0	-3.072622	-6.319645	-1.508622
19	1	0	-5.056704	-5.501861	-1.004085
20	6	0	-1.746629	-5.907842	-1.515281
21	1	0	-3.363920	-7.313963	-1.831018
22	6	0	-3.385043	4.163181	-0.633770
23	6	0	-3.983942	5.366598	-0.955858
24	16	0	-1.648367	4.267178	-0.857180
25	6	0	-3.072583	6.346082	-1.393080
26	1	0	-5.056329	5.519613	-0.902236
27	6	0	-1.746489	5.934664	-1.406597
28	1	0	-3.363995	7.345749	-1.698374
29	16	0	1.648363	4.267183	-0.857172
30	6	0	3.072577	6.346092	-1.393062
31	6	0	3.385040	4.163188	-0.633761
32	6	0	3.983937	5.366609	-0.955839
33	1	0	3.363987	7.345760	-1.698351
34	6	0	4.032893	2.955901	-0.169479
35	1	0	5.056323	5.519627	-0.902213
36	6	0	3.657474	1.643725	-0.319830
37	16	0	5.565367	3.103460	0.706557
38	6	0	4.595883	0.710383	0.227021
39	1	0	2.756061	1.350821	-0.847503
40	6	0	5.701481	1.364242	0.815191
41	6	0	4.599745	-0.713359	0.206376
42	6	0	6.785760	0.685048	1.396776
43	6	0	5.698398	-1.378824	0.794436
44	6	0	3.662623	-1.636078	-0.360493
45	6	0	6.773378	-0.711053	1.406367
46	16	0	5.562427	-3.115519	0.652629
47	6	0	4.033292	-2.951269	-0.226040
48	1	0	2.765431	-1.333239	-0.889748
49	6	0	3.385564	-4.150139	-0.712358
50	6	0	3.984291	-5.347945	-1.054704
51	16	0	1.648841	-4.249800	-0.937823

52	6	0	3.072630	-6.319636	-1.508646
53	1	0	5.056712	-5.501849	-1.004112
54	6	0	1.746635	-5.907839	-1.515289
55	1	0	3.363929	-7.313952	-1.831046
56	8	0	-7.798665	-1.456626	1.938415
57	8	0	-7.799671	1.419803	1.964983
58	8	0	7.799663	1.419811	1.964992
59	8	0	7.798671	-1.456616	1.938411
60	6	0	-9.059457	1.338994	1.278724
61	1	0	-9.743797	1.985039	1.832462
62	1	0	-8.960817	1.705549	0.250027
63	1	0	-9.437637	0.312287	1.269734
64	6	0	-7.916567	-1.385238	3.368720
65	1	0	-6.996765	-1.740393	3.848279
66	1	0	-8.131914	-0.363283	3.695044
67	1	0	-8.745160	-2.045109	3.633869
68	6	0	9.059471	1.338984	1.278775
69	1	0	9.437643	0.312274	1.269810
70	1	0	8.960866	1.705528	0.250071
71	1	0	9.743796	1.985032	1.832528
72	6	0	7.916522	-1.385261	3.368722
73	1	0	8.131847	-0.363309	3.695077
74	1	0	6.996708	-1.740436	3.848241
75	1	0	8.745114	-2.045127	3.633886
76	6	0	-0.681181	6.816336	-1.814271
77	1	0	-1.102358	7.747198	-2.192450
78	6	0	0.681176	6.816338	-1.814268
79	1	0	1.102351	7.747201	-2.192446
80	6	0	1.746484	5.934668	-1.406590
81	6	0	-0.681162	-6.782414	-1.937783
82	1	0	-1.102327	-7.706736	-2.331694
83	6	0	0.681169	-6.782413	-1.937786
84	1	0	1.102333	-7.706735	-2.331698

The optimized energy for the macrocycle (**5**) was obtained to be – 5179.86 a.u.

## Reference 23 in full

M. J. Frisch, G. W. Trucks, H. B. Schlegel, G. E. Scuseria, M. A. Robb, J. R. Cheeseman, G. Scalmani, V. Barone, B. Mennucci, G. A. Petersson, H. Nakatsuji, M. Caricato, X. Li, H. P. Hratchian, A. F. Izmaylov, J. Bloino, G. Zheng, J. L. Sonnenberg, M. Hada, M. Ehara, K. Toyota, R. Fukuda, J. Hasegawa, M. Ishida, T. Nakajima, Y. Honda, O. Kitao, H. Nakai, T. Vreven, J. A. Montgomery, Jr. J. E. Peralta, F. Ogliaro, M. Bearpark, J. J. Heyd, E. Brothers, K. N. Kudin, V. N. Staroverov, R. Kobayashi, J. Normand, K. Raghavachari, A. Rendell, J. C. Burant, S. S. Iyengar, J. Tomasi, M. Cossi, N. Rega, J. M. Millam, M. Klene, J. E. Knox, J. B. Cross, V. Bakken, C. Adamo, J. Jaramillo, R. Gomperts, R. E. Stratmann, O. Yazyev, A. J. Austin, R. Cammi, C. Pomelli, J. W. Ochterski, R. L. Martin, K. Morokuma, V. G. Zakrzewski, G. A. Voth, P. Salvador, J. J. Dannenberg, S. Dapprich, A. D. Daniels, O. Farkas, J. B. Foresman, J. V. Ortiz, J. Cioslowski and D. J. Fox, *Gaussian 09, Revision A.02*, Gaussian Inc., Wallingford CT, 2009.